Available online at www.sciencedirect.com
ScienceDirect
Journal of Power Sources 165 (2007) 342–346
JOURNAL OF POWER SOURCES
www.elsevier.com/locate/jpowsour

Short communication

Performance of a miniaturized silicon reformer-PrOx-fuel cell system

Oh Joong Kwon, Sun-Mi Hwang, Je Hyun Chae, Moo Seong Kang, Jae Jeong Kim *

Research Center for Energy Conversion and Storage, School of Chemical and Biological Engineering, Seoul National University, Shillim-dong, Kwanak-gu, Seoul 151-742, Republic of Korea

Received 16 August 2006; accepted 14 November 2006
Available online 16 January 2007

Abstract

A fuel cell made with silicon is operated with hydrogen supplied by a reformer and a preferential oxidation (PrOx) reactor those are also made with silicon. The performance and durability of the fuel cell is analyzed and tested, then compared with the results obtained with pure hydrogen. Three components of the system are made using silicon technologies and micro electro-mechanical system (MEMS) technology. The commercial Cu-ZnO-Al_2O_3 catalyst for the reformer and the Pt-Al_2O_3 catalyst for the PrOx reactor are coated by means of a fill-and-dry method. A conventional membrane electrode assembly composed of a 0.375 mg cm^{-2} PtRu/C catalyst for the anode, a 0.4 mg cm^{-2} Pt/C catalyst for the cathode, and a Nafion^{TM} 112 membrane is introduced to the fuel cell. The reformer gives a 27 cm^3 min^{-1} gas production rate with 3177 ppm CO concentration at a 1 cm^3 h^{-1} methanol feed rate and the PrOx reactor shows almost 100% CO conversion under the experimental conditions. Fuel cells operated with this fuel-processing system produce 230 mW cm^{-2} at 0.6 V, which is similar to that obtained with pure hydrogen.

Keywords: Reformer; Preferential oxidation reactor; Reformed hydrogen; Fuel cell

1. Introduction

Fuel cells and solar cells are the core technologies for future energy systems and have been studied extensively since the end of the 20th century [1,2]. Fuel cells are more favourable than solar cells because the technologies used for fuel cells are closer to commercial realization than solar cell technology. Energy for automobiles, residential power generators, and portable electric devices are the main fields in which fuel cells may be adopted [3–6]. The use of fuel cells for portable devices is the most promising of these applications.

To introduce fuel cells to portable electric devices, various systems such as direct methanol fuel cells (DMFCs) and polymer electrolyte membrane fuel cells (PEMFCs) with sodium borohydride or fuel processors have been studied. DMFCs are relatively simple systems, but their power density is too low for high-power devices such as notebook computers. On the other hand, PEMFCs have high power densities but the systems are complex because hydrogen is a gas at the operating conditions [7]. Regardless of the type of fuel cell, the important point in their application to portable electric devices is how to make the system sufficiently small and compact. Various ideas to miniaturize these systems with different materials have been proposed, and the fuel cell system made with silicon being one of them.

Silicon has already been applied in the fabrication of micro sensors, micro actuators and lab-on-a-chip units to make the corresponding conventional system smaller [8–10]. Recently, silicon has also been introduced in the fabrication of fuel processors and fuel cells [11–13]. Small silicon-based reformers have generated sufficient hydrogen to operate a notebook computer, and silicon-based fuel cells have shown the possibility of replacing graphite-based conventional fuel cells. When reformers and fuel cells are combined, each system affects the other. Thus, investigation of the mutual effects of reformers and fuel cells is essential for the development of silicon-based fuel processors and fuel cell systems [14,15].

This study focuses on the operation of combined systems, composed of a reformer, a preferential oxidation (PrOx) reactor and a fuel cell. Silicon-based reformers, PrOx reactors, and fuel cells are fabricated and their performance is tested individually to evaluate their own characteristics. The three components are connected serially to analyze the mutual effects and to compare the results with those obtained from a fuel cell operated with pure hydrogen.

* Corresponding author. Tel.: +82 2 880 8863; fax: +82 2 888 2705.
E-mail address: jjkimm@snu.ac.kr (J.J. Kim).

0378-7753/$ – see front matter © 2006 Elsevier B.V. All rights reserved.
doi:10.1016/j.jpowsour.2006.11.074

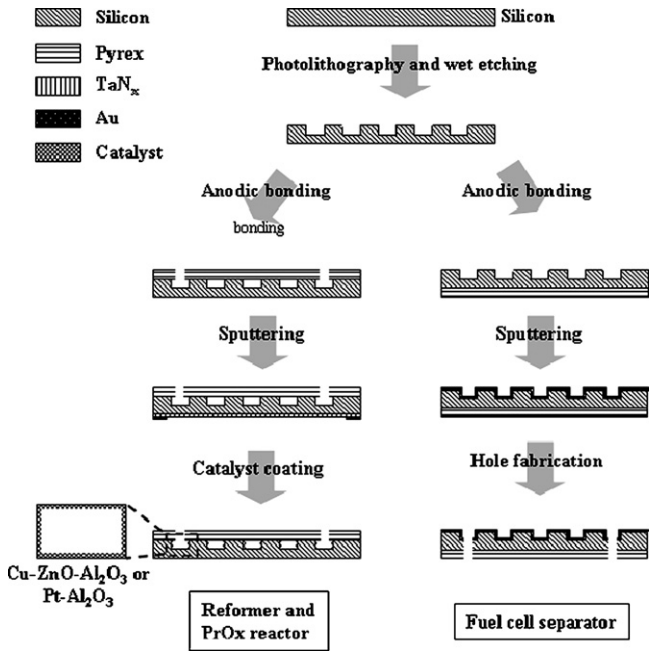

Fig. 1. Fabrication process of reformer, PrOx reactor, and fuel cell separator.

2. Fabrication

(1 1 0) silicon wafers and Pyrex were the main materials used for fabrication of the reformer, PrOx reactor, and fuel cell. A schematic diagram of the reformer, PrOx reactor, and fuel cell separator fabrication processes is given in Fig. 1. A silicon wafer was first wet oxidized to form a SiO_2 etch mask, then lithography was performed to transfer the channel pattern on silicon wafer. Wet etching was performed with a KOH etchant at 80 °C for 2 h, and a 240 μm deep channel was formed [16]. The wet etched silicon wafer was bonded with Pyrex for both reactors and fuel cell separators [17]. Pyrex was used to seal the micro channels except at the inlet and outlet for the reactors, and to increase the hardness of the fuel cell separators as reported in a previous paper. After the silicon wafers were bonded to the Pyrex, a thin film heater and gold current collectors were deposited by direct current sputtering on the silicon sides of both of the reactors and the fuel cell separator. The thin film heaters were composed of 80 nm thick TaN_x heating material, a few nm of tantalum as an adhesion layer and a 300 nm gold contact pad. The current collectors on the fuel cells were made up of tantalum adhesion layer and a 500 nm gold layer.

After finishing the reactor fabrication, the catalysts were coated inside the micro channels for the steam reforming of methanol (SRM) and the PrOx reaction. A Cu-ZnO-Al_2O_3 reforming catalyst of MDC-3 from Süd-Chemie was used for the SRM reaction and a 5 wt.% Pt-Al_2O_3 catalyst from Johnson Matthey for the PrOx reaction were coated on their respective reactors. Both catalysts were ball-milled with deionized water to make a slurry. The catalyst slurries were coated inside the micro channels by a fill-and-dry method. Calcination was carried out at 300 °C for the Cu-ZnO-Al_2O_3 catalyst and at 500 °C for the Pt-Al_2O_3 catalyst for 3 h, and afterwards a drying process was performed for 5 days. Fig. 2 shows the enhanced scanning electron microscope (FESEM) coating profiles of the Cu-ZnO-Al_2O_3 and Pt-Al_2O_3 catalysts, and photographs of the reformer and PrOx reactor both with and without packaging. The volumes of the reformer and the PrOx reactor were 1.03 and 0.57 cm^3, respectively.

A conventional membrane electrode assembly (MEA) was prepared for the silicon-based miniaturized fuel cell. Carbon paper without wet-proof treatment (Toray TGPH-090, 260 μm) were used as the gas diffusion layer (GDL), and 0.375 mg cm^{-2} PtRu/C (HISPEC 5000, Johnson Matthey) was introduced as the anode catalyst and 0.4 mg cm^{-2} Pt/C (C1-40, E-TEK) as the cathode catalyst. PtRu/C was adopted as an anode catalyst instead of Pt/C to reduce the catalyst poisoning effect caused by

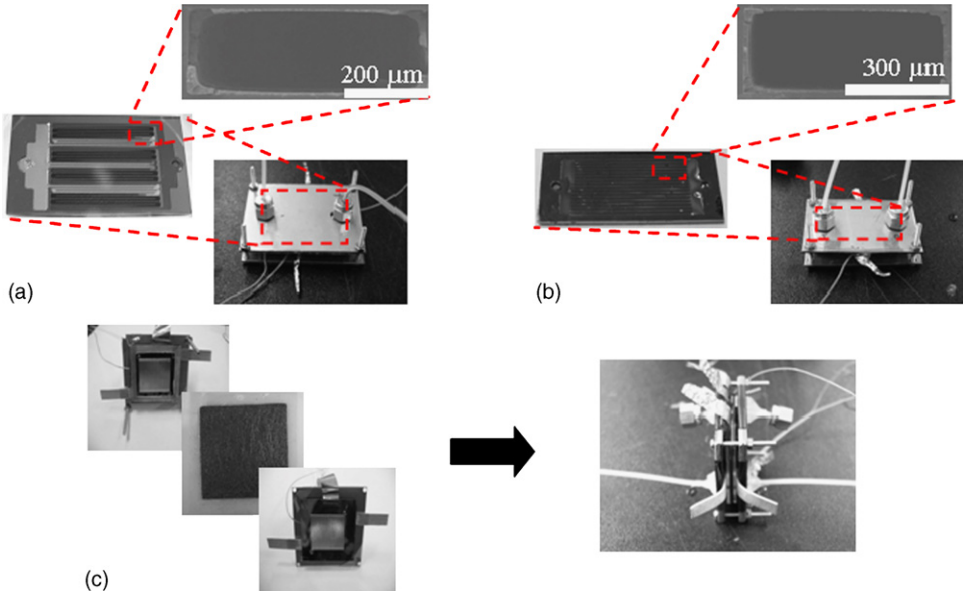

Fig. 2. Photographs and FESEM images of: (a) reformer, (b) PrOx reactor and (c) fuel cell.

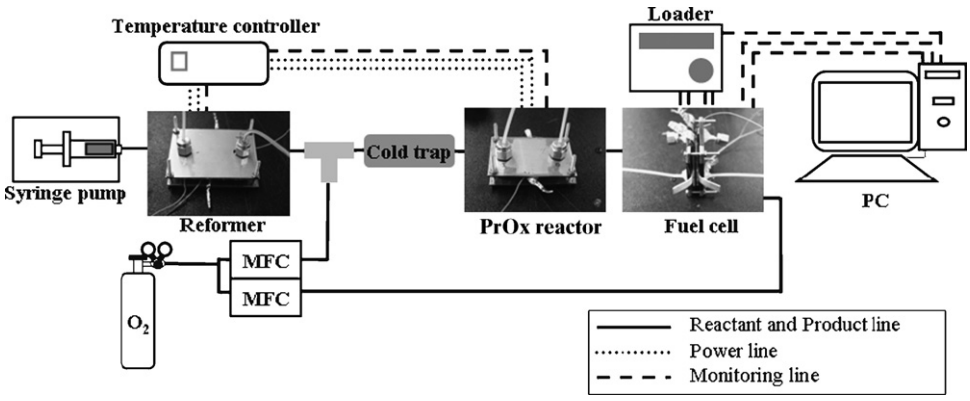

Fig. 3. Schematic diagram of experimental setup.

CO that might still exist in the reformed gas even after the PrOx reaction. To load the catalyst, a spray coating method with an air-brush was employed. On both catalysts layers, 0.3 mg cm^{-2} of Nafion was impregnated. An assembled single fuel cell is shown in Fig. 2. The active area of the MEA was 4 cm^2, and the total volume of one single cell, including end plates, was 2.25 cm^3.

3. Experimental

Before combining the reformer, PrOx reactor and fuel cell, each component was tested individually to determine its individual performance. The temperatures of the reformer and the PrOx reactor were controlled by thin film heaters, deposited on to the back of each reactor, and a temperature controller that was composed of a power supply, a relay and a proportional-integral-differential (PID) algorithm program. The flow rate of product gas was measured with a digital flowmeter and the composition of the product gas was determined with a gas chromatograph (Varian CP 4900).

The polarization and power density curves of the fuel cell when operated with pure hydrogen and oxygen were recorded with an electrical load system (EL-200P, Deagil electronics Co. Ltd.). The fuel cell was activated by cycling the potential with pure hydrogen and oxygen, and analysis was carried out under atmospheric pressure. The flow rates of the hydrogen and oxygen were regulated with mass flowmeter/controllers (EL-Flow®, Bronkhorst High-Tech).

After performance testing, the components were connected in series to operate the fuel cell with hydrogen generated by the reformer and purified in the PrOx reactor. A schematic diagram of the experimental setup is given in Fig. 3. Methanol solution, with a steam-to-carbon (S/C) ratio of one, was supplied with a syringe pump. The test results of the fuel cell operated with reformed hydrogen, were compared with those obtained with pure hydrogen and oxygen.

4. Results and discussion

The reformer, shown in Fig. 2(a), consisted of four parallel channels, which had a width of 600 μm and a depth of 240 μm. Inside each channel, a Cu-ZnO-Al_2O_3 catalyst was coated with a total weight of 20 mg. The temperature of reformer was maintained at 280 °C by means of a TaN_x thin film heater. The performance of the reformer is presented in Fig. 4. Methanol was supplied at a S/C ratio of one and with a feed rate that varied between 1 and 2 $cm^3\ h^{-1}$. The reformer gave 100% conversion at a 1 $cm^3\ h^{-1}$ methanol feed rate to yield a 27.5 $cm^3\ min^{-1}$ gas production rate, which corresponds to 3.2 W_t (thermal watt). When the potential of the fuel cell is 0.6 V and hydrogen utilization is 100%, the power reduces to 1.6 W.

The CO concentration is reported in Fig. 4. The reformer produces 3170 ppm and 3420 ppm at a 1 and 2 $cm^3\ h^{-1}$ methanol feed rate, respectively. Although this is relatively low compared with the results for a conventional reformer, both CO levels are still too high to be applied to fuel cell. The CO concentration should be reduced to below 10 ppm [18].

To remove CO to a level that is applicable to fuel cells, a PrOx reactor was connected to the reformer. The PrOx reactor had parallel channels that were 600 μm wide and 240 μm deep and into which Pt-Al_2O_3 was coated by a fill-and-dry method. Oxygen was supplied between the reformer and the PrOx reactor. A cold trap was located before the PrOx reactor to remove any unreacted methanol solution and water. The results obtained from this reformer and PrOx system are given in Fig. 5. The CO concentration was analyzed by varying the operation temperature of the PrOx reactor with 1 and 2 $cm^3\ h^{-1}$ methanol feed rates. Both tests show a similar trend, in which the CO concentra-

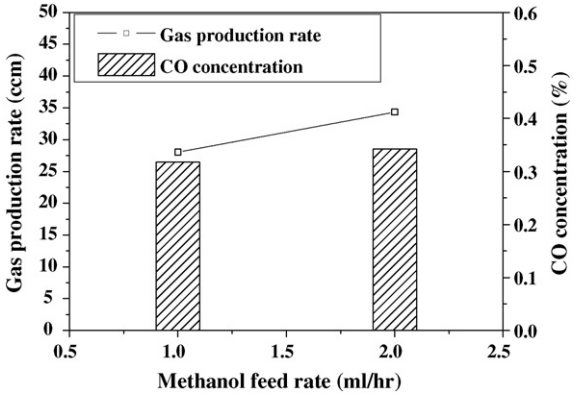

Fig. 4. Performance of reformer; gas production rate and CO concentration according to methanol feed rate.

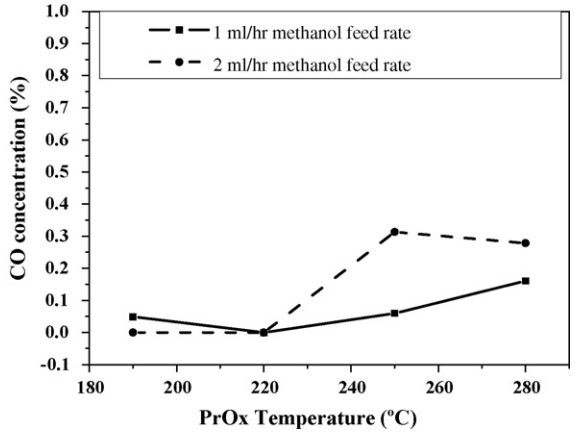

Fig. 5. CO concentration vs. PrOx operation temperature at 1 and 2 $cm^3\ h^{-1}$ methanol feed rates.

tion increases after reaching the minimum value as the operation temperature is increased. This behaviour arises because the PrOx reaction is exothermic. After passing the optimum temperature range, a reverse reaction occurs. The minimum CO concentration is nearly 0 ppm at 220 °C and is independent of the methanol feed rate, as shown in Fig. 5. This means that the CO concentration is below the detection limit of the gas chromatographic system. Thus, the PrOx reactor is inserted between the reformer and fuel cell at an operation temperature of 220 °C.

The performance of the miniaturized fuel cells made with silicon separators was analyzed with pure hydrogen and oxygen before the performance was measured with reformed hydrogen supplied by the miniaturized reformer and PrOx reactor system. 0.375 mg cm^{-2} of PtRu/C (0.25 mg cm^{-2} based on Pt weight) was coated as an anode catalyst instead of a Pt/C catalyst to reduce the catalyst poisoning effect that might occur due to the remaining CO after the PrOx reaction. The *I–V* and power density curves measured with hydrogen and oxygen flow rates of 20 $cm^3\ min^{-1}$ are shown in Fig. 6. The *I–V* curve decreases and the power density curve increases smoothly, then both drop dramatically at a current density of 650 mA cm^{-2}. The latter observation is due to a lack of hydrogen at the anode. A flow rate of 20 $cm^3\ min^{-1}$ of hydrogen corresponds to 657 mA cm^{-2} with a 4 cm^2 active area. The power density at 0.6 V is 210 mW cm^{-2}. Even though this value is lower than that for a fuel cell with a

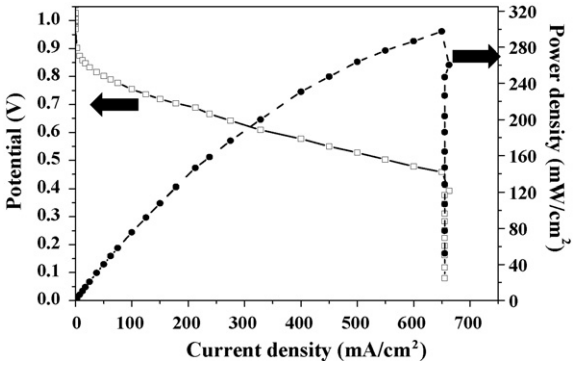

Fig. 6. *I–V* and power density curves of single fuel cell with pure hydrogen and oxygen.

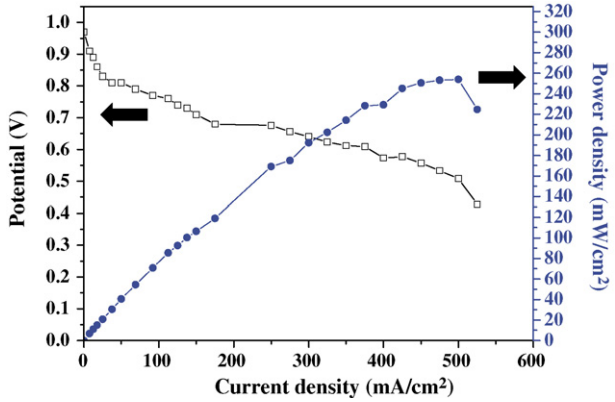

Fig. 7. *I–V* and power density curves of single fuel cell with hydrogen generated by reformer and PrOx reactor.

conventional graphite plate, the small volume compensates for the low power density. The volumetric power density, including the end plates, is 360 mW cm^{-3}, which is comparable with that of a conventional fuel cell.

A miniaturized fuel cell was operated with reformed hydrogen, to compare the results with those obtained with pure hydrogen and to monitor the effect of CO effect on the anode catalyst. The operating conditions of the reformer and the PrOx reactor were the same as those detailed above, namely, 280 and 220 °C, respectively, with a 1 $cm^3\ h^{-1}$ methanol feed rate. Pure oxygen was used at the cathode, and the flow rate was controlled at 20 $cm^3\ min^{-1}$. The *I–V* and power density curves are given in Fig. 7. The performance with reformed hydrogen is close to that with pure hydrogen, as shown in Fig. 6. Even at 0.6 V, the power density is 20 mW cm^{-2} higher, viz., 230 mW cm^{-2}. This means that the CO is successfully removed at the PrOx reactor and the reformed hydrogen does not affect the performance of the fuel cell.

The results of a short-term durability test, shown in Fig. 8, give further clear evidence that CO is successfully removed and reformed hydrogen does cause any adverse effects. The test was carried out with reformed hydrogen for 20 h at 250 mA cm^{-2}. The potential is 0.67 V and is maintained during the experiment. Given that a very low CO concentration of around 10 ppm

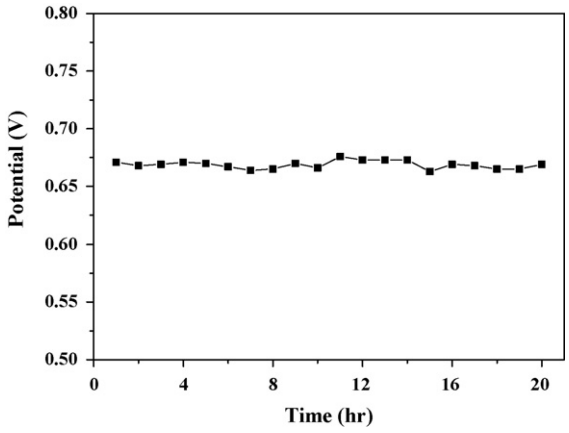

Fig. 8. Durability test of single fuel cell at 250 mA cm^{-2} with hydrogen generated by reformer and purified by PrOx reactor.

can deteriorate the anode catalyst, the stable potential over 20 h means that the PrOx reactor and the PtRu/C catalyst play their respective roles very effectively.

5. Conclusions

A miniaturized reformer, PrOx reactor and fuel cell, which are the components to operate a fuel cell with reformed hydrogen, are successfully made with silicon fabrication technologies and a fill-and-dry catalyst coating method. The reformer gives 100% conversion at a methanol feed rate of 1 $cm^3\,h^{-1}$ at 280 °C, with a CO concentration of 3170 ppm. This high CO concentration generated by the reformer is reduced to under the detection limit with a PrOx reactor operated at 220 °C. With pure hydrogen, the fuel cell delivers a power density of 210 $mW\,cm^{-2}$ at 0.6 V. When this is converted to volumetric power density, it is similar to the performance of a conventional fuel cell.

After analyzing the performance of each component, the components were connected serially to operate the fuel cell with reformed hydrogen. A power density of 230 $mW\,cm^{-2}$ at 0.6 V is obtained. A durability test gives more clear evidence that the fuel cell can be operated with reformed hydrogen which is generated and cleaned by a silicon-based reformer and a PrOx reactor. The fuel cell maintains its potential of 0.67 V for 20 h at 250 $mA\,cm^{-2}$.

Acknowledgements

This work was supported by KOSEF through the Research Center for Energy Conversion and Storage (RCECS), the Seoul Renewable Energy Research Consortium (Seoul RERC) and the Inter-University Semiconductor Research Center (ISRC).

References

[1] L. Carrette, K.A. Friedrich, U. Stimming, Fuel Cells 1 (2001) 5–39.
[2] P. Costamagna, S. Srinivasan, J. Power Sources 102 (2001) 242–252.
[3] Y. Kamiya, K. Narusawa, Proceedings of the International Workshop on Next Generation Power Systems for Automobiles, 2000, pp. 80–91.
[4] J.P. Mayers, H.L. Maynard, J. Power Sources 109 (2002) 76–88.
[5] M. Müller, C. Müller, F. Gromball, M. Wolfle, W. Menz, Microsyst. Technol. 9 (2003) 159–162.
[6] C. Hebling, A. Heinzel, Fuel Cells Bull. (July) (2002) 8–12.
[7] A.S. Arico, S. Srinivasan, V. Antonucci, Fuel Cells 1 (2001) 133–161.
[8] T. Cui, J. Fang, A. Zheng, F. Jones, A. Reppnd, Sens. Actuators B Chem. 71 (2000) 228–231.
[9] S. Tanaka, K.-S. Chang, K.-B. Min, D. Satoh, K. Yoshida, M. Esashi, Chem. Eng. J. 101 (2004) 143–149.
[10] J. Cheng, M.A. Shoffner, G.E. Hivichia, L.J. Kricka, P. Wilding, Nucleic Acids Res. 24 (1996) 380–385.
[11] J. Yu, P. Cheng, Z. Ma, B. Yi, J. Power Sources 124 (2003) 40–46.
[12] O. Kwon, S.-M. Hwang, J.-G. Ahn, J. Kim, J. Power Sources 156 (2006) 253–259.
[13] S.C. Kelley, G.A. Deluga, W.H. Smyrl, Electrochem. Solid State Lett. 3 (2000) 407–409.
[14] A.V. Pattekar, M.V. Kothare, J. Microelectromech. S. 13 (2004) 7–18.
[15] M.U. Kopp, A.J. Mello, A. Manz, Science 280 (1998) 1046–1048.
[16] H. Hamatsu, M. Nagase, K. Kurihara, K. Iwadate, K. Murase, Microelectron. Eng. 27 (1995) 71–74.
[17] M.A. Schmidt, Proc. IEEE 86 (1998) 1575–1585.
[18] S. Jimenez, J. Soler, R.X. Valenzuela, L. Daza, J. Power Sources 151 (2005) 69–73.